arXiv:cond-mat/0103093v1 [cond-mat.mes-hall] 5 Mar 2001

Kondo resonant spectra in coupled quantum dots

Tomosuke Aono[1] and Mikio Eto[2,3]
[1] *The Institute of Physical and Chemical Research (RIKEN),*
2-1 Hirosawa, Wako-shi, Saitama 351-0198 Japan
[2] *Faculty of Science and Technology, Keio University,*
3-14-1 Hiyoshi, Kohoku-ku, Yokohama 223-8522 Japan
[3] *Department of Applied Physics/DIMES, Delft University of Technology,*
Lorentzweg 1, 2628 CJ Delft, The Netherlands

(February 1, 2008)

The Kondo effect in coupled quantum dots is investigated from the viewpoint of transmission spectroscopy using the slave-boson formalism of the Anderson model. The antiferromagnetic spin-spin coupling J between the dots is taken into account. Conductance G through the dots connected in a series is characterized by the competition between the dot-dot tunneling coupling V_C and the level broadening Δ in the dots (dot-lead coupling). When $V_C/\Delta < 1$, the Kondo resonance is formed between each dot and lead, which is replaced by a spin-singlet state in the dots at low gate voltages. The gate voltage dependence of G has a sharp peak of $2e^2/h$ in height in the crossover region between the Kondo and spin-singlet states. The sharp peak of G survives when the energy levels are different between the dots. When $V_C/\Delta > 1$, the "molecular levels" between the Kondo resonant states appear; the Kondo resonant peaks are located below and above the Fermi level in the leads at low gate voltages. The gate voltage dependence of G has a broad peak, which is robust against J. The broad peak splits into two peaks when the energy levels are different, reflecting the formation of the asymmetric molecular levels between the Kondo resonant states.

73.23.Hk72.15.Qm, 85.35.Be

I. INTRODUCTION

Recently the Kondo effect has been observed in semiconductor quantum dots connected to external leads by tunneling barriers.[1–4] The Kondo effect makes a resonant state at the Fermi level in the leads when the number of electrons in the dot is odd.[5–12] The resonant width is given by the Kondo temperature T_K. This results in (i) the unitary limit of the linear conductance through the dot $G = 2e^2/h$ at low temperatures ($T \ll T_K$) (Ref. 5) and (ii) the zero-bias peak of the differential conductance $dI/dV_{\rm sd}$ with the width of T_K under finite source-drain voltages.[9]

In this paper, we theoretically examine the Kondo resonant state in double quantum dots connected in a series, as will be shown in Fig. 1. We consider one level in each quantum dot, often referred to as an "artificial atom".[13,14] At $T \gg T_K$, the transport properties of such systems have been investigated by several experiments,[15–18] from a view point of the formation of an "artificial molecule." The molecular orbitals between the two dots have been observed,[17,18] which reflect the coherent coupling between the dots (V_C in Fig. 1). When the double dot system accommodates two electrons, the coherent coupling and intra-dot interaction U make many-body states[19,20]. The ground state is a spin singlet. The excitation energy to a spin-triplet state is given by

$$J = \frac{V_C}{2}\left[\sqrt{(U/V_C)^2+16} - (U/V_C)\right] \approx 4V_C^2/U, \tag{1}$$

when $U \gg V_C$. The ground state is an "entangled" state between two localized spins, which has attracted new interest for the application to quantum computing.[21] At $T \ll T_K$, the two elements V_C and J would lead to rich structures of the Kondo resonant state in this system.

A useful tool to elucidate the Kondo resonance is the slave-boson formalism of the Anderson model with $U \to \infty$.[22–26] In the case of a single quantum dot, the dot state is spin-up $f_\uparrow^\dagger|0\rangle$, spin-down $f_\downarrow^\dagger|0\rangle$, or empty $b^\dagger|0\rangle$ ($f_\uparrow^\dagger f_\uparrow + f_\downarrow^\dagger f_\downarrow + b^\dagger b = 1$). In the mean-field approximation, b and $b^\dagger$ are replaced by a real c-number, $b^\dagger = b = b_0$. The density of states for pseudo fermions per spin is[27]

$$\rho_f(\omega) = -\frac{\rm Im}{\pi}\frac{1}{\omega - \widetilde{E} + {\rm i}\widetilde{\Delta}} = \frac{1}{\pi}\frac{\widetilde{\Delta}}{(\omega-\widetilde{E})^2+\widetilde{\Delta}^2}. \tag{2}$$

In the Kondo regime where one electron exists in the dot ($b_0^2 \ll 1$, $f_\uparrow^\dagger f_\uparrow + f_\downarrow^\dagger f_\downarrow \cong 1$), the density of states $\rho_f(\omega)$ is half filled and, hence, the center of the resonant state $\widetilde{E}$ is matched with the Fermi level. The width $\widetilde{\Delta}$ is the Kondo temperature

$$T_{K,1} = \frac{\Delta}{\pi} \exp(\pi E^*/\Delta), \tag{3}$$

where Δ is the level broadening, $\pi\rho|V|^2$, with the density of states ρ in the external leads and the dot lead tunneling coupling V. E^* is the renormalized dot-level, $E^* = V_g + \Delta/\pi \ln(D\pi/\Delta)$ with the gate voltage V_g and the bandwidth D in the leads.[28] Therefore this method is suitable to examine how the Kondo resonant state is formed. When the number of electrons in the dot is less than unity (valence fluctuating regime), the center of the resonance moves above the Fermi level. The resonant width increases from T_K to Δ, as the number of electrons in the dot decreases. However, the mean-field approximation is not quantitatively accurate in the valence fluctuating regime.

The Kondo effect on the transport properties in coupled dot systems have been studied by several theoretical methods.[29–34] In our previous paper,[35] we have applied the slave boson mean-field theory to the double dot system in the absence of the antiferromagnetic spin-spin coupling J. We have shown that the Kondo resonance is determined by the competition between the dot-dot tunneling coupling V_C and dot-lead coupling Δ. The resonant state has two peaks below and above the Fermi level for $V_C/\Delta > 1$, whereas it has a single peak at the Fermi level for $V_C/\Delta < 1$. In consequence, the linear-conductance G through the double dots as a function of the gate voltage is qualitatively different between the two cases.

Extending our calculations, Georges and Meir[36] have pointed out the importance of the spin-spin coupling J. At low-gate voltages, the coupling becomes relevant and makes a spin-singlet state in the two dots. Then the Kondo resonance between dots and leads is destroyed. Izumida and Sakai[34] have examined the same problem using the numerical renormalization group (NRG) method. A similar situation was investigated for dilute magnetic systems, which is known as the two impurity Kondo problem.[37–42] When the antiferromagnetic coupling J, the origin of which is the Ruderman-Kittel-Kasuya-Yosida interaction, increases from zero, electronic states of two magnetic impurities exhibit the first-order phase transition from the Kondo state to the spin-singlet state at $J \sim T_{K,1}$. The magnetic susceptibility diverges at the transition. The phase transition changes into a crossover in the case of $V_C \neq 0$.[40,41] In coupled quantum dots, J is given by Eq. (1) whereas $T_{K,1}$ increases as the gate voltage increases as in Eq. (3).

As indicated by the previous work[34,36], the interplay of Δ, V_C, and J results in various transport properties. They are observable by experiments since these parameters can be controlled in quantum dot systems. The physical origins of the transport properties, however, are difficult to understand by the NRG method[34] and by the conventional argument using the phase shift.[36] In this paper, we look directly at the Kondo resonant state in the presence of spin-spin coupling J. The effect of J can be understood in terms of the transmission spectrum, just as in our previous work in the absence of J. We will show that even for $J \neq 0$, electron transport is characterized by the competition between the dot-dot tunneling coupling V_C and the dot-lead coupling Δ. When $V_C/\Delta < 1$, the coupling J is essentially important. G has a sharp peak of $2e^2/h$ in height, as a function of gate voltage, which stems from the coexistence of the Kondo coupling and spin-singlet coupling. When $V_C/\Delta > 1$, the transport properties are robust against J. These results are explained by only one criterion, whether the transmission spectrum has double peaks. Hence our argument is much simpler than the one based on the phase shift.[36] In addition, the transmission spectrum by itself is directly observable in the differential conductance under finite source-drain voltages, as suggested by Aguado and Langreth.[43] Further, we generalize our calculations to asymmetric double dot systems. Some preliminary results have been reported in Ref. 44.

The organization of this paper is as follows. In Sec. II, the model Hamiltonian for a coupled quantum dot system is introduced. We explain the slave boson mean-field theory and derive the expression of the conductance through the dots. In Sec. III, we briefly review electron transport through symmetric double dots in the absence of J. The transmission spectra are discussed in detail. In Sec. IV, we investigate electron transport through coupled dots in the presence of J. In Sec. V, the electron transport through asymmetric double dots is examined. Conclusions and discussion follow in Sec. VI.

II. MODEL AND METHOD

A. Model

Let us consider coupled quantum dots as shown in Fig. 1. Two dots couple to each other with V_C, and to external leads with V. Each dot has a single energy level E_α ($\alpha = \mathrm{L}, \mathrm{R}$). We denote the energy difference, $E_L - E_R$, by ΔE. A common gate V_g is attached to the dots to control E_α; we define $V_g = (E_L + E_R)/2$. We assume that the intradot

Coulomb interaction U is sufficiently large so that (i) the double occupancy of electrons in each dot is forbidden, but (ii) the antiferromagnetic spin coupling exists between the quantum dots due to the virtual double occupancy in a dot, $J\boldsymbol{S}_L \cdot \boldsymbol{S}_R$ with J $(= 4V_C^2/U)$ [see Eq. (1)] and the spin operator $\boldsymbol{S}_\alpha(\alpha = L, R)$. The interdot Coulomb interaction is neglected. The temperature is set to be zero.

We adopt the $(N = 2)$-fold degenerate Anderson model with the antiferromagnetic SU(N) spin interactions, represented by the slave-boson formalism.[36,39] We introduce the slave boson operator $b_\alpha^\dagger$, which creates an empty state and fermion operator $f_{\alpha m}^\dagger$, which creates a singly occupied state with spin $m = -j, -(j-1), ..., j-1, j(2j+1 = N)$ in dot $\alpha = L, R$, under the constraint of $\widehat{Q}_\alpha \equiv n_\alpha + b_\alpha^\dagger b_\alpha = 1$ with $n_\alpha = \sum_m f_{\alpha m}^\dagger f_{\alpha m}$. The annihilation operator of an electron in dot α is rewritten as $C_{\alpha m} = b_\alpha^\dagger f_{\alpha m}$.[22–26]

The Hamiltonian is

$$\mathcal{H} = \mathcal{H}_0 + \mathcal{H}_{\text{dot-lead}} + \mathcal{H}_{\text{dot-dot}} + \mathcal{H}_J + \sum_{\alpha=\text{L,R}} \lambda_\alpha(\hat{Q}_\alpha - 1). \tag{4}$$

The first term on the right-hand side of Eq. (4) represents electrons in the leads and dots;

$$\mathcal{H}_0 = \sum_{\substack{\alpha=\text{L,R}\\ k,\, m}} E(k) c_{\alpha k m}^\dagger c_{\alpha k m} + \sum_{\substack{\alpha=\text{L,R}\\ m}} E_\alpha f_{\alpha m}^\dagger f_{\alpha m}. \tag{5}$$

The operator $c_{\alpha k m}^\dagger$ creates an electron in lead α with energy $E(k)$ and spin m. The second and third terms on the right hand side of Eq. (4) describe the dot-lead tunneling coupling and the dot-dot tunneling coupling, respectively

$$\mathcal{H}_{\text{dot-lead}} = \frac{V}{\sqrt{N}} \sum_{\alpha,k,m} c_{\alpha k m}^\dagger f_{\alpha m} b_\alpha^\dagger + \text{H.c.}, \tag{6}$$

$$\mathcal{H}_{\text{dot-dot}} = \frac{V_C}{N} \sum_m b_L^\dagger f_{Lm} f_{Rm}^\dagger b_R + \text{H.c.} \tag{7}$$

The term H_J gives the antiferromagnetic spin-spin interaction

$$\mathcal{H}_J = \frac{J}{N} \sum_{m,n} f_{Rm}^\dagger f_{Lm} f_{Ln}^\dagger f_{Rn} + \text{H.c.} \tag{8}$$

The constraint of $\widehat{Q}_\alpha = 1$ is taken into account by the last term on the right-hand side of Eq. (4) with the Lagrange multiplier λ_α.

B. Mean-Field Approximation

Let us now make the following two assumption to treat the Hamiltonian (4) within the mean-field theory.[23,39] First, the slave-boson operators b_α and $b_\alpha^\dagger$ are replaced by a constant c-number b_α. This approximation is exact in the limit of $N \to \infty$ when $J = 0$; it corresponds to the calculation to the lowest order in the $1/N$ expansion.[22–24] Second, we also treat the spin-spin coupling (8) by the mean-field theory. It is decoupled by a parameter κ,

$$\kappa = \frac{J}{N} \sum_m \langle f_{Rm}^\dagger f_{Lm} \rangle, \tag{9}$$

which characterizes the antiferromagnetic order between the spins in the dots. Then we obtain the following mean-field Hamiltonian;

$$\begin{aligned} \mathcal{H}_0 = &\sum_{\substack{\alpha=\text{L,R}\\ k,\, m}} E(k) c_{\alpha k m}^\dagger c_{\alpha k m} + \sum_m (f_{Lm}^\dagger f_{Rm}^\dagger) \begin{pmatrix} \widetilde{E}_L & \widetilde{V}_\text{C} + \kappa \\ \widetilde{V}_\text{C} + \kappa & \widetilde{E}_R \end{pmatrix} \begin{pmatrix} f_{Lm} \\ f_{Rm} \end{pmatrix} \\ &+ \frac{V}{\sqrt{N}} \sum_{\alpha,k,m} b_\alpha \left(c_{\alpha k m}^\dagger f_{\alpha m} + f_{\alpha m}^\dagger c_{\alpha k m} \right) + \sum_{\alpha=\text{L,R}} \lambda_\alpha (b_\alpha^2 - 1) + \frac{1}{J}\kappa^2, \end{aligned} \tag{10}$$

where $\widetilde{E}_\alpha = E_\alpha + \lambda_\alpha$ and $\widetilde{V}_\mathrm{C} = \bar{b}_L \bar{b}_R V_C$ with $\bar{b}_\alpha = b_\alpha/\sqrt{N}$.

From this Hamiltonian, we can calculate the ground state energy. Minimizing the ground state energy, we determine five parameters b_α, λ_α ($\alpha = \mathrm{L}, \mathrm{R}$) and κ self consistently. (See Appendix A.) In general, the self-consistent equations have two solutions; one is $\widetilde{\Delta}_\alpha = 0$ ($b_\alpha = 0$) and $\kappa = J/2$, and the other is $\widetilde{\Delta}_\alpha \neq 0$. The former means that electrons in the dots are isolated from the leads and make a spin-singlet state. The latter corresponds to the coherent couplings between dots and leads. We determine the ground state by comparing the energies of these solutions.

C. Conductance

Next we derive the expression of the conductance G. Current I through the coupled dots under a source-drain voltage V_sd is given by a charge transfer through the central tunneling barrier

$$I = \frac{-ieV_C}{\hbar} \sum_m \left(\langle c^\dagger_{Lm} c_{Rm} \rangle - \langle c^\dagger_{Rm} c_{Lm} \rangle \right), \tag{11}$$

where $\langle ... \rangle$ represents the Keldysh-Green function. By the mean-field approximations, $\langle c^\dagger_{Lm} c_{Rm} \rangle = b_L b_R \langle f^\dagger_{Lm} f_{Rm} \rangle$, where $\langle f^\dagger_{Lm} f_{Rm} \rangle$ can be calculated using the Hamiltonian (10). (See Appendix B.)

Evaluating the Keldysh-Green functions, we obtain the expression of the conductance $G \equiv \lim_{V_\mathrm{sd} \to 0} I/V_\mathrm{sd}$,

$$G = \frac{2e^2}{h} T(\omega = 0), \tag{12}$$

formally in the same form as the Landauer formulae.[35] The transmission probability $T(\omega)$ through the two dots is

$$T(\omega) = \frac{4\widetilde{\Delta}_L \widetilde{\Delta}_R t^2}{\left[(\omega - \widetilde{E}_L - i\widetilde{\Delta}_L)(\omega - \widetilde{E}_R - i\widetilde{\Delta}_R) - t^2\right] \left[(\omega - \widetilde{E}_L + i\widetilde{\Delta}_L)(\omega - \widetilde{E}_R + i\widetilde{\Delta}_R) - t^2\right]}, \tag{13}$$

with $\widetilde{\Delta}_\alpha = \bar{b}_\alpha^2 \Delta$ ($\alpha = L, R$) and $t = \widetilde{V}_C + \kappa$. We choose $\omega = 0$ at the Fermi level in the leads.

III. SYMMETRIC DOUBLE DOTS WITHOUT J

We begin with a symmetric double dot system $E_L = E_R$ in the absence of the spin-spin coupling $J = 0$. Because of the symmetry between the two dots $\bar{b}_L = \bar{b}_R \equiv \bar{b}$, $n_L = n_R \equiv n/2$, $\lambda_L = \lambda_R$, and $\widetilde{E}_L = \widetilde{E}_R \equiv \widetilde{E}$. $\kappa = 0$ due to the absence of J. Then the expression of the transmission probability $T(\omega)$ in Eq. (13) is simplified to

$$T(\omega) = \frac{4\widetilde{\Delta}^2 \widetilde{V}_\mathrm{C}^2}{\left[\left(\omega - (\widetilde{E} + \widetilde{V}_\mathrm{C})\right)^2 + \widetilde{\Delta}^2\right] \left[\left(\omega - (\widetilde{E} - \widetilde{V}_\mathrm{C})\right)^2 + \widetilde{\Delta}^2\right]}, \tag{14}$$

with $\widetilde{\Delta} = \bar{b}^2 \Delta$ and $\widetilde{V}_\mathrm{C} = \bar{b}^2 V_C$. The parameter $\widetilde{V}_\mathrm{C}$ characterizes the effective dot-dot coupling. Note that $\widetilde{V}_\mathrm{C}/\widetilde{\Delta} = V_C/\Delta$.

The line shape of $T(\omega)$ is determined by the parameter of V_C/Δ.[35] In Fig. 2, $T(\omega)$ is plotted as a function of $\omega/\widetilde{\Delta}$. When $V_C/\Delta < 1$, $T(\omega)$ has a single peak at $\omega = \widetilde{E}$ [Fig. 2(a)], whereas when $V_C/\Delta > 1$, $T(\omega)$ has two maxima at $\omega = \widetilde{E} \mp \sqrt{\widetilde{V}_\mathrm{C}^2 - \widetilde{\Delta}^2}$ [Fig. 2(c)]. When $V_C/\Delta = 1$, $T(\omega)$ has a flat-topped single peak as shown in Fig. 2(b).

The dotted line in Fig. 3(a) represents the conductance as a function of the gate voltage when $V_C/\Delta < 1$. For sufficiently low gate voltages, the Fermi level in the leads is located at the peak of $T(\omega)$ [the case of $V_g/\Delta = -2$ is indicated by the arrow in Fig. 2(a)]. In this case, each dot accommodates one electron and forms the Kondo resonant state with conduction electrons in a lead. The electron transport is determined by the hopping between the two Kondo resonant states. Thus G is proportional to V_C^2 and independent of the gate voltage. As the gate voltage increases, the position of the Fermi level shifts downwards [the cases of $V_g/\Delta = 0$ and 1 in Fig. 2(a)]. The number of electrons in the dots n decreases monotonically from 2 to 0 (valence fluctuating regime). As a result, G decreases with increasing the gate voltage.

The dotted line in Fig. 4(a) represents the conductance as a function of the gate voltage when $V_C/\Delta > 1$. For low gate voltages, the Fermi level in the leads is located at the center of $T(\omega)$ [the case of $V_g/\Delta = -7$ in Fig. 2(c)], and thus the conductance G is considerably suppressed. As the gate voltage increases, the Fermi level shifts downwards [the case of $V_g/\Delta = -4$ in Fig. 2(c)], which increases G. At a gate voltage of $V_g \approx 0$, the Fermi level is just on the bonding peak and, thus, the conductance G has the maximum value of $2e^2/h$. On increasing the gate voltage further, the Fermi level shifts downwards further [the case of $V_g/\Delta = 5$ in Fig. 2(c)], which leads to a decrease in G.

In summary, when $V_C/\Delta < 1$, the electron transport is characterized by electronic states in each dot below the Kondo temperature whereas, when $V_C/\Delta > 1$, it is characterized by the formation of molecular levels of the Kondo resonant states. In the recent work,[43] Aguado and Langreth have argued that these molecular levels are directly observable in the differential conductance under finite source-drain voltages.

We next mention V_g dependence of the peak width $\widetilde{\Delta}$ of the Kondo resonances. When $V_C/\Delta \ll 1$,

$$\widetilde{\Delta} = \begin{cases} T_{\mathrm{K}} & (V_g < 0) \\ \widetilde{\Delta}_{\mathrm{VF}} \equiv \Delta/2\left(\frac{1}{2} + \frac{2}{\pi}\arctan(V_g/\Delta)\right) & (0 < V_g\ ) \end{cases}, \tag{15}$$

where T_{K} is the Kondo temperature for the coupled dots,

$$T_{\mathrm{K}} = T_{K,1}\exp\left(\frac{V_C}{\Delta}\arctan\frac{V_C}{\Delta}\right)/\sqrt{1+(V_C/\Delta)^2}. \tag{16}$$

$T_{K,1}$ is given by Eq. (3). T_{K} increases exponentially with V_g or V_C.[36] When $V_C/\Delta \gg 1$,

$$\widetilde{\Delta} = \begin{cases} T_{\mathrm{K}} & (V_g < -V_C/2) \\ \frac{\Delta}{2V_C}(V_g + V_C/2) & (-V_C/2 < V_g < V_C/2) \\ \widetilde{\Delta}_{\mathrm{VF}} & (V_C/2 < V_g) \end{cases}. \tag{17}$$

(See Appendix C.)

IV. SYMMETRIC DOUBLE DOTS WITH J

Now we discuss a symmetric double dot system, $E_L = E_R$, in the presence of the spin-spin coupling J. When the coupling J is strong enough, the Kondo coupling between a dot and lead is destroyed and a spin-singlet state appears between the dots. First we make a rough estimation of $J = J_c$, where the crossover between the Kondo and spin-singlet states takes places. The ground-state energy ϵ_{gs} in Eq. (A11) is given by

$$\epsilon_{\mathrm{gs}} = V_g - \frac{2}{\pi}\widetilde{\Delta} - \frac{\kappa^2}{J} - \frac{2\widetilde{E}\widetilde{\Delta}}{\Delta}, \tag{18}$$

where $\widetilde{\Delta}_{L,R} \equiv \widetilde{\Delta}$, $\widetilde{E}_{L,R} \equiv \widetilde{E}$, and $n_{L,R} \equiv n/2$. Here we have used the self-consistent equations in Appendix A. The last term is negligible when $n \sim 2$. We consider two simple situations; (i) Kondo state without spin-singlet ordering ($\kappa = 0$), $\epsilon_{\mathrm{gs}} = V_g - \frac{2}{\pi}\widetilde{\Delta}$, and (ii) spin-singlet state without the Kondo effect ($\widetilde{\Delta} = 0$ and $\kappa = J/2$), $\epsilon_{\mathrm{gs}} = V_g - J/4$. The crossover between (i) and (ii) takes place at $J_{\mathrm{c}}/\widetilde{\Delta} = 8/\pi \cong 2.54$. If $V_C \to 0$, $\widetilde{\Delta} \to T_{K,1}$ and thus $J_{\mathrm{c}}/T_{K,1} = 2.54$. This is consistent with the NRG result of the two impurity Kondo problem, $J_{\mathrm{c}}/T_{K,1} \cong 2.2$.[37] When $V_C/\Delta = 0.11$ and $J_{\mathrm{c}}/\Delta = 2.1 \times 10^{-3}(U/\Delta = 21.2)$, $J_{\mathrm{c}}/\Delta = 2.55$ is in good agreement with the recent NRG calculation of the coupled dot system[34] that gives $J_{\mathrm{c}}/T_{K,1} = 2.65$.

In coupled quantum dots, J is given by $4V_C^2/U$. $U/\Delta = 4 \times 10^2$ is assumed in this paper. We investigate the gate voltage dependence of G with fixed J. With decreasing V_g, the Kondo effect becomes weaker, as indicated in Eq. (3), and thus J is relatively stronger compared with $\widetilde{\Delta}$. At sufficiently low gate voltages, a spin-singlet state appears that destroys the Kondo effect.

A. Transmission probability

In the present case, the transmission probability $T(\omega)$ is given by

$$T(\omega) = \frac{4\widetilde{\Delta}^2 t^2}{\left[\left(\omega - (\widetilde{E} + t)\right)^2 + \widetilde{\Delta}^2\right]\left[\left(\omega - (\widetilde{E} - t)\right)^2 + \widetilde{\Delta}^2\right]}, \tag{19}$$

where $t = \widetilde{V}_{\mathrm{C}} + \kappa$, $\widetilde{V}_{\mathrm{C}} = \bar{b}^2 V_C$, and $\widetilde{\Delta} = \bar{b}^2\Delta$. This result is the same as the one without J [Eq. (14)] if the dot-dot coupling $\widetilde{V}_{\mathrm{C}}$ is replaced by t. Then the line shape of $T(\omega)$ qualitatively depends on whether $t/\widetilde{\Delta} = V_C/\Delta + \kappa/\widetilde{\Delta}$ is larger than unity.

B. Weak dot-dot coupling case

First we discuss electron transport when $V_C/\Delta < 1$. The solid line in Fig. 3(a) represents V_g dependence of G, while the solid and dotted lines in Fig. 3(b) represent V_g dependence of κ and $\widetilde{\Delta}$, respectively ($V_C/\Delta = 0.3, J/\Delta = 9.0 \times 10^{-4}$). For sufficiently low gate voltages, $\kappa = J/2$ and $\widetilde{\Delta} = 0$, indicating a complete spin-singlet state, which results in $G = 0$. With increasing V_g, the Kondo effect is stronger. As a consequence, $\widetilde{\Delta}$ becomes larger, whereas κ becomes smaller. At high gate voltages, G is identical to the one without J (dotted line). Here the spin-spin coupling J is weak enough compared with the Kondo effect. Between these two regions, G has a sharp peak of $2e^2/h$ in height. At this peak, both of the Kondo effect $\widetilde{\Delta}$ and spin-singlet coupling κ coexist [see the inset in Fig. 3(b)]. This peak structure of G is consistent with the NRG calculations.[34]

The calculated results of the G-V_g curve can be understood by Eq. (19). At high gate voltages, $\kappa/\widetilde{\Delta} \ll 1$ so that $t/\widetilde{\Delta} = V_C/\Delta + \kappa/\widetilde{\Delta} \simeq V_C/\Delta$; the plot of G is similar to the one of $J = 0$. With decreasing V_g, $\kappa/\widetilde{\Delta}$ increases and thus $t/\widetilde{\Delta}$ becomes larger. On the right hand side of the sharp peak of G, $t/\widetilde{\Delta} < 1$ and hence $T(\omega)$ has a single peak. At $\kappa/\widetilde{\Delta} = 1 - V_C/\Delta$, $t/\widetilde{\Delta} = 1$ and $T(\omega = 0) = 1$, resulting in $G = 2e^2/h$. With decreasing V_g further, split peaks of $T(\omega)$ suppress G. At a certain gate voltage, the Kondo states disappear and a spin-singlet state appears ($\kappa = J/2$ and $\widetilde{\Delta} = 0$).

From the results given above, the origin of the peak of G is explained as follows. The Kondo resonant state is formed by the coherent coupling between the dot and the lead while the spin-singlet state is formed by the coherent coupling between the two dots. When these two states coexist, the left and right leads are connected via a coherent channel. Electrons transfer through this channel and as a result, $T(\omega = 0) = 1$.

We find that the width of the sharp peak is roughly given by V_C. This implies that the crossover region between the spin-singlet state and the Kondo state becomes wider as V_C increases. It is consistent with the results by Sakai *et al.*[40,41] for the two-impurity Kondo problem. (See also Refs. 34,36.)

C. Strong dot-dot coupling case

Next we discuss electron transport when $V_C/\Delta > 1$. The solid line in Fig. 4(a) represents V_g dependence of G; the solid and dotted lines in Fig. 4(b) represent V_g dependence of κ and $\widetilde{\Delta}$, respectively ($V_C/\Delta = 10.0, J/\Delta = 1.0$). For this case, the gate voltage dependence of G is fairly robust against J except that the region of $G = 0$ for low gate voltages. When $G = 0$, $\kappa = J/2$ and $\widetilde{\Delta} = 0$ (spin-singlet state in the dots) as in the case of $V_C/\Delta < 1$. Both of κ and $\widetilde{\Delta}$ change gradually against the gate voltage (there is a simple relation of $2\kappa/J = 1/2 - \widetilde{\Delta}/\Delta$, see Appendix C). These results contrast to the ones for the weak dot-dot coupling case.

The robustness of G against J is explained as follows. At the top of the broad peak of G, $n \simeq 1$ as seen in the previous section. On the right-hand side of the peak, $n < 1$ and spin-spin coupling J is not relevant. On the left-hand side of the peak, $n > 1$ and the antiferromagnetic interaction becomes more effective with decreasing V_g. However, the transition from the Kondo states to the spin-singlet state takes place at quite a low gate voltage because the Kondo temperature T_K [Eq. (16)] is much larger than $T_{\mathrm{K},1}$ for strong dot-dot coupling. In addition, $t/\widetilde{\Delta}$ is always larger than unity when $V_C/\Delta > 1$. Thus the spin coupling J does not introduce qualitatively new features in expression (19).

D. Intermediate region of V_C/Δ

Finally, we show V_g dependence of G by changing the magnitude of V_C/Δ in Fig. 5. As V_C increases, (i) the height of the plateau increases, (ii) the sharp peak of G broadens, and (iii) the position of the sharp peak of G shifts to larger V_g. When $V_C/\Delta > 1$, the peak position is fixed at $V_g \sim 0$. At the peak of G, $n = 2$ when $V_C/\Delta \ll 1$ while $n = 1$ when $V_C/\Delta \gg 1$; n decreases gradually from 2 to 1 as V_C increases. In conclusion, electron transport and electronic states in the dots change continuously from the weak to strong dot-dot coupling regions.

V. ASYMMETRIC DOUBLE QUANTUM DOTS

In this section, we discuss the effects of the energy difference $\Delta E = E_L - E_R$ between the dots. First we describe the case of $V_C/\Delta < 1$. In Fig. 6, the gate voltage dependence of G is shown for $\Delta E = 0$ (thin dotted line) and

$\Delta E \neq 0$ (thick dotted line) in the absence of J. These plots show that ΔE has no effect on the height of G when the gate voltage is low enough and both of the dots accommodate one electron. This is because the dot-lead coupling makes the Kondo resonant state at the Fermi level in the leads, irrespective of the position of the dot levels. The single peak of the transmission probability $T(\omega)$ is located at the Fermi level, as discussed in Fig. 2(a). As a result, G is insensitive to ΔE. In the presence of J, the gate voltage dependence of G is shown for $\Delta E = 0$ (thin solid line) and $\Delta E \neq 0$ (thick solid line). The sharp peak of G appears, but the peak height is less than $2e^2/h$.

Next, we describe the case of $V_C/\Delta > 1$. In Fig. 7, the gate voltage dependence of G is shown for $\Delta E = 0$ (thin dotted line) and $\Delta E \neq 0$ (thick dotted line) in the absence of J. For low gate voltages, $n_L = n_R = 1$ and G is independent of ΔE as in the case of $V_C/\Delta < 1$. In the valence fluctuating regime, where n decreases as V_g increases, $n_L \neq n_R$, and hence, electron transport depends on ΔE prominently. The broad peak of G splits into two peaks. They are less than $2e^2/h$ in height. At the left-hand peak, n_L decreases from unity to zero with increasing V_g while $n_R \simeq 1$. At the right-hand peak, n_R decreases from unity to zero while $n_L \simeq 0$. These peaks are understood by the Kondo resonance between a molecular orbital in the dimer and leads. One molecular orbital has the amplitude mainly in the left dot, and the other in the right dot. The peak heights of G are determined by the amplitude of the orbitals in the other dot. Note that the gate voltage dependence of G is fairly robust against J as in the case of $\Delta E = 0$ (compare the thick dotted and thick solid lines in Fig. 7).

Finally, we show the intermediate region of V_C/Δ in Fig. 8. When $V_C/\Delta \ll 1$, G has a sharp peak. As V_C/Δ increases, the sharp peak broadens and a weak peak develops at $V_g \sim \Delta E/2$. The width of the weak peak is $\sim \Delta$. The line shapes of these two peaks become similar to each other. Electron transport changes continuously from the weak to strong dot-dot coupling regions, as discussed in Fig. 5 in the case of $\Delta E = 0$.

VI. CONCLUSIONS AND DISCUSSION

We have investigated the conductance through coupled quantum dots in series, as a function of the gate voltage, below the Kondo temperature. Electron transport is characterized by the ratio of V_C/Δ. When $V_C/\Delta < 1$, a plateau of G appears because each dot forms the Kondo resonant state with conduction electrons in a lead and G is determined by the hopping between the Kondo states. For low gate voltages, they are replaced by the spin-singlet state and $G = 0$. A sharp peak of G appears with the height of $2e^2/h$, which is due to a coherent electron transport brought by the cooperation between the Kondo and spin-singlet states. When the energy levels are different in the dots, the sharp peak survives, but the peak height is less than $2e^2/h$. When $V_C/\Delta > 1$, the molecular levels between the Kondo resonant states appear. The gate voltage dependence of G has a broad peak. The antiferromagnetic spin coupling is ineffective, compared with the case of $V_C/\Delta < 1$, because (i) the Kondo temperature of a coupled dot is large and (ii) the transmission probability always has two peaks. When the energy levels are different in the dots, the conductance G has two peaks, reflecting asymmetric molecular levels.

We should mention the validity of the mean-field approximation. First, the mean-field theory predicts the first-order transition between the Kondo and spin-singlet states when $V_C/\Delta < 1/\pi$;[39] it is an artifact of the mean field theory, because the NRG results show that when $V_C \neq 0$, the transition is always smooth.[40,41] For the present problem of coupled dot systems, this artifact appears on the left-hand side of the sharp peak of G; a discontinuous jump of G is seen for $V_C/\Delta = 0.2$ in Fig. 5. Second, in the valence fluctuating regime, the fluctuations around the mean field of the slave boson are not negligible. Hence, our calculations are not enough for quantitative discussion.

In real coupled quantum dots, the intersite Coulomb energy, $U_{\rm int} n_L n_R$, is present. Then the ground-state energy $E_{\rm g,int}$ is given by

$$E_{\rm g,int} = E_{\rm gs} + U_{\rm int}(1 - b_L^2)(1 - b_R^2), \qquad (20)$$

in the mean-field approximation. Equation (20) indicates that the intersite Coulomb energy raises the dot levels E_L and E_R effectively. As a result, the valence fluctuating regime is extended and the Kondo regime shifts to lower V_g. Note that we have assumed that the on-site Coulomb interaction U is infinite, and thus, $U_{\rm int} \ll U$.

When $U_{\rm int}$ is large enough, the coupled dots cannot accommodate more than one electron. This situation has been investigated by Pohjola *et al.*[31]. In this case, the coupled dots is regarded as a single quantum dot with two levels when the dot-dot tunneling is large. Pohjola *et al.* have found a splitting of the Kondo resonance due to the level difference ΔE between the two dots. The one peak is on the Fermi level E_F and the other is located at $E_F + \Delta E$. This is in contrast to the present case in which the split peaks are located below and above E_F.

Finally, we comment on an asymmetric dot-lead coupling case, $\Delta_L \neq \Delta_R$. This asymmetry introduces the following two effects. First, the maximum of the conductance is less than $2e^2/h$ by a geometrical asymmetry $4\Delta_L\Delta_R/(\Delta_L + \Delta_R)^2$.[5] Second, the difference of dot-lead coupling $\delta\Delta \equiv (\Delta_L - \Delta_R)/2$ introduces a difference in the number of electrons between the dots, resulting in $\widetilde{E}_L \neq \widetilde{E}_R$. Electronic states are, therefore, asymmetric; the situation is similar to the case of $E_L \neq E_R$ discussed in Sec. V. [Equation (A9) in Appendix A is modified by replacing $\widetilde{\Delta}_0 \to \widetilde{\Delta}_0 + \bar{b}_1^2\,\delta\Delta$ and $\widetilde{\Delta}_1 \to \widetilde{\Delta}_1 + \bar{b}_0^2\,\delta\Delta$. The latter modification means that $n_L \neq n_R$ when $\delta\Delta \neq 0$.]

ACKNOWLEDGMENTS

We acknowledge Yu. V. Nazarov for fruitful comments. T.A. is supported by the Special Postdoctoral Researchers Program of RIKEN. Numerical calculations were performed on the workstation in the Computer Information Center, RIKEN.

APPENDIX A: DERIVATION OF THE GROUND STATE ENERGY

First, we review a single impurity model with the impurity level E.[23,25,26] We start from the following mean-field Hamiltonian $\mathcal{H}$

$$\mathcal{H} = \sum_{k,\,m} E(k) c_{km}^\dagger c_{km} + \sum_m \widetilde{E} f_m^\dagger f_m + \frac{Vb}{\sqrt{N}} \sum_{k,m} \left(c_{km}^\dagger f_m + f_m^\dagger c_{km} \right) + \lambda(b^2 - 1) \tag{A1}$$

with $\widetilde{E} = E + \lambda$ and b is the mean field value of the slave boson.

The free energy F of the system is given by

$$F = -\frac{2}{\beta} \int \mathrm{d}\omega \ln(1 + e^{-\beta\omega}) \bar{\rho}(\omega) + \lambda(b^2 - 1), \tag{A2}$$

where $\bar{\rho}(\omega)$ is the density of states, which is given by the retarded Green function $G_r(\omega)$ of electrons in the dot

$$\bar{\rho}(\omega) = \frac{\mathrm{Im}}{\pi} G_r(\omega) = \frac{\mathrm{Im}}{\pi} \frac{1}{\omega - \widetilde{E} - \Sigma(\omega)}, \tag{A3}$$

with the self-energy $\Sigma(\omega)$

$$\Sigma(\omega) = \frac{b^2 V^2}{N} \sum_k \frac{1}{\omega - E(k) + i\eta} = -i\pi \frac{b^2 V^2}{N} \rho(\omega) \equiv -i\widetilde{\Delta}\Phi(\omega). \tag{A4}$$

Here $\rho(\omega)$ is the density of states of conduction electrons in a lead, $\rho = \rho(\omega = 0)$, $\Phi(\omega) = \rho(\omega)/\rho$, and $\widetilde{\Delta} = \pi\rho b^2 V^2/N$. To derive Eq. (A4), we have assumed that $\rho(\omega)$ varies smoothly when compared with $\widetilde{\Delta}$.

By the substitution of Eqs. (A3) and (A4) into Eq. (A2) and integration by parts, the free energy (A2) becomes

$$F = \frac{N}{\pi} \mathrm{Im} \int_{-\infty}^{\infty} \mathrm{d}\omega f(\omega) \Phi(\omega) \ln(\omega - \xi) + \lambda(b^2 - 1), \tag{A5}$$

with $\xi = \widetilde{E} + i\widetilde{\Delta}$.

If the leads has a wide flat band of width $2D$, $\Phi(\omega) = 1 (-D < \omega < D)$, the free energy is

$$F = \frac{N}{\pi} \mathrm{Im} \int_{-D}^{D} \mathrm{d}\omega f(\omega) \ln(\omega - \xi) + \lambda(b^2 - 1). \tag{A6}$$

At zero temperature, this yields

$$F = \frac{N}{\pi} \mathrm{Im} \left\{ \xi \left(\ln\left(\frac{\xi}{D}\right) - 1 \right) \right\} + \lambda(b^2 - 1). \tag{A7}$$

An extension to the coupled dot system is straightforward. The free energy is

$$F = \frac{N}{\pi} \mathrm{Im} \sum_{P=\pm} \int_{-D}^{D} \mathrm{d}\omega f(\omega) \ln(\omega - \xi_P) + \sum_{\alpha=\mathrm{L,R}} \lambda_\alpha (b_\alpha^2 - 1) + \frac{N}{J}\kappa^2, \tag{A8}$$

with

$$\xi_P = \widetilde{E}_0 + i\widetilde{\Delta}_0 + P\sqrt{(\widetilde{E}_1 + i\widetilde{\Delta}_1)^2 + t^2}. \tag{A9}$$

Here $\widetilde{E}_{0,1} = (\widetilde{E}_L \pm \widetilde{E}_R)/2$, $\widetilde{\Delta}_{0,1} = \bar{b}_{0,1}^2 \Delta$ with $\bar{b}_{0,1}^2 = (\bar{b}_L^2 \pm \bar{b}_R^2)/2$, and $t = V_C\sqrt{\bar{b}_0^4 - \bar{b}_1^4} + \kappa$. ξ_P are the eigenvalues of the matrix given by

$$\begin{pmatrix} \widetilde{E}_L + i\widetilde{\Delta}_L & \widetilde{V}_\mathrm{C} + \kappa \\ \widetilde{V}_\mathrm{C} + \kappa & \widetilde{E}_R + i\widetilde{\Delta}_R \end{pmatrix}. \tag{A10}$$

Then the ground-state energy $E_\mathrm{gs} = N\epsilon_\mathrm{gs}[= F(T=0)]$ is written as

$$\epsilon_\mathrm{gs} = 2(\widetilde{E}_0 - E^*)(\bar{b}_0^2 - 1/2) + 2(\widetilde{E}_1 - \Delta E)\,\bar{b}_1^2 + \frac{1}{J}\kappa^2 + \frac{1}{\pi}\sum_{P=\pm} \mathrm{Im}\,\left[\xi_P\left(\ln\frac{\pi\xi_P}{\Delta} - 1\right)\right], \tag{A11}$$

where $E^* = V_g + \Delta/\pi \ln(D\pi/\Delta)$ with the bandwidth D in the leads.[28] In experiments, E^* can be controlled by the gate voltage V_g (we redefine E^* as V_g).

Minimizing the ground-state energy (A11), we determine five parameters, $b_\alpha,\ \lambda_\alpha$ $(\alpha = \mathrm{L}, \mathrm{R})$, and κ, self-consistently. The self-consistent equations are

$$2\left(\widetilde{E}_0 - V_g\right) + \frac{1}{\pi}\sum_P \mathrm{Im}\left[\left(i\Delta + \frac{P\,\bar{b}_0^2\,t\,V_C}{\sqrt{\,\bar{b}_0^4 - \bar{b}_1^4}\sqrt{(\widetilde{E}_1 + i\widetilde{\Delta}_1)^2 + t^2}}\right)\ln\frac{\pi\xi_P}{\Delta}\right] = 0, \tag{A12}$$

$$2\left(\widetilde{E}_1 - \frac{\Delta E}{2}\right) + \frac{1}{\pi}\sum_P \mathrm{Im}\left[\frac{i\widetilde{E}_1\Delta - \bar{b}_0^2\left(\Delta^2 + V_C^2 + \kappa V_C/\sqrt{\,\bar{b}_0^4 - \bar{b}_1^4}\right)}{\sqrt{(\widetilde{E}_1 + i\widetilde{\Delta}_1)^2 + t^2}} P\ln\frac{\pi\xi_P}{\Delta}\right] = 0, \tag{A13}$$

$$2\left(\bar{b}_0^2 - 1/2\right) + \frac{1}{\pi}\sum_P \mathrm{Im}\left[\ln\frac{\pi\xi_P}{\Delta}\right] = 0, \tag{A14}$$

$$2\bar{b}_1^2 + \frac{1}{\pi}\sum_P \mathrm{Im}\left[\frac{(\widetilde{E}_1 + i\widetilde{\Delta}_1)}{\sqrt{(\widetilde{E}_1 + i\widetilde{\Delta}_1)^2 + t^2}} P\ln\frac{\pi\xi_P}{\Delta}\right] = 0, \tag{A15}$$

$$\frac{2\kappa}{J} + \frac{1}{\pi}\sum_P \mathrm{Im}\left[\frac{t}{\sqrt{(\widetilde{E}_1 + i\widetilde{\Delta}_1)^2 + t^2}} P\ln\frac{\pi\xi_P}{\Delta}\right] = 0. \tag{A16}$$

APPENDIX B: EXPRESSION OF CURRENT

In this appendix, we derive the expression of the current using the real-time functional integral method. The alternative derivation is given in Ref. 45, which is based on the equation of motions for the Green functions. We take $\hbar = 1$ in this appendix.

All of the physical quantities can be obtained in principle by calculating the time evolution of the density matrix $\rho(t)$

$$\rho(t) = U^\dagger(t)\rho_\mathrm{init.}U(t), \tag{B1}$$

where $\rho_\mathrm{init.}$ is the initial density matrix and $U(t)$ is the time evolution kernel of the Hamiltonian H

$$U(t) = T\exp\left(-iH(t)\right), \tag{B2}$$

using the time ordering product T.

Corresponding to Eq. (B1), we introduce the generating functional $W[\boldsymbol{j}_1, \boldsymbol{j}_2]$,[46,47]

$$\exp\left(W\left[\boldsymbol{j}_1, \boldsymbol{j}_2\right]\right) = \mathrm{Tr}\ U^{j_1\,\dagger}(t)\rho_\mathrm{init.}U^{j_2}(t), \tag{B3}$$

where $U^j(t)$ is the time evolution kernel of the Hamiltonian $H^j = H - \bar{\boldsymbol{j}} \cdot \boldsymbol{f} - \bar{\boldsymbol{f}} \cdot \boldsymbol{j}$ with $\bar{\boldsymbol{j}} = (\bar{j}_{Lm}, \bar{j}_{Rm})$, $\bar{\boldsymbol{f}} = (\bar{f}_{Lm}, \bar{f}_{Rm})$ and their conjugates $\boldsymbol{j}$ and $\boldsymbol{f}$. Equation (B3) is evaluated using the real-time functional integral method, which is the functional integral on the Keldysh contour;[48–51] the suffix "1" and "2" in j correspond to the upper and lower branches of the Keldysh contour, respectively.

For the Hamiltonian (10), Eq. (B3) is given by the following functional integral on the degrees of freedom of electrons in the dots;[52]

$$\exp\left(W[J]\right) = \int \mathcal{D}\boldsymbol{f}\mathcal{D}\bar{\boldsymbol{f}}\ \exp\left(\sum_{m=\pm 1/2} \int \mathrm{d}\omega\ \bar{\boldsymbol{F}}\, G^{-1}\, \boldsymbol{F} - \boldsymbol{J} \cdot \bar{\boldsymbol{F}} - \bar{\boldsymbol{F}} \cdot \boldsymbol{J}\right) \tag{B4}$$

$\bar{\boldsymbol{F}} = \left(\bar{f}_{+;Lm}(\omega),\ \bar{f}_{-;Lm}(\omega),\ \bar{f}_{+;Rm}(\omega),\ \bar{f}_{-;Rm}(\omega)\right)$ and $\bar{\boldsymbol{J}} = (\bar{j}_{-;Lm}(\omega),\ \bar{j}_{+;Lm}(\omega),\ \bar{j}_{-;Rm}(\omega),\ \bar{j}_{+;Rm}(\omega))$ with $f_+ = (f_1 + f_2)/2$, $f_- = f_1 - f_2$, $j_+ = (j_1 + j_2)/2$, $j_- = j_1 - j_2$. The matrix G^{-1} is the inverse of the Green functions:

$$G^{-1}(\omega) = \begin{pmatrix} 0 & G^{-1}_{\mathrm{r,L}}(\omega) & 0 & t \\ G^{-1}_{\mathrm{a,L}}(\omega) & \widetilde{\Delta}_L f_L(\omega) & t & 0 \\ 0 & t & 0 & G^{-1}_{\mathrm{r,R}}(\omega) \\ t & 0 & G^{-1}_{\mathrm{a,R}}(\omega) & \widetilde{\Delta}_R f_R(\omega) \end{pmatrix}, \tag{B5}$$

with the Fermi function $f_\alpha(\omega)$ of the electrodes with the chemical potential μ_α and the retarded and advanced Green function $G^{-1}_{\mathrm{r,a},\ \alpha}$ ($\alpha = \mathrm{L},\ \mathrm{R}$) of electrons in the dots:

$$G^{-1}_{\mathrm{r},\alpha}(\omega) = \omega + \widetilde{E}_\alpha + i\widetilde{\Delta}_\alpha, \tag{B6}$$

$$G^{-1}_{\mathrm{a},\alpha}(\omega) = \omega + \widetilde{E}_\alpha - i\widetilde{\Delta}_\alpha. \tag{B7}$$

After integrating over the degrees of freedom of electron in the dots, the generating functional W is finally given by $G(\omega)$,

$$W = -\sum_{m=\pm 1/2} \int d\omega\ \bar{\boldsymbol{J}}\ G(\omega)\ \boldsymbol{J}. \tag{B8}$$

The current I (11) is rewritten as

$$I = -ie\widetilde{V}_{\mathrm{C}} \sum_m \int d\omega \left(\langle \bar{f}_{+;Lm} f_{+;Rm}(\omega)\rangle - \langle \bar{f}_{+;Rm} f_{+;Lm}(\omega)\rangle\right). \tag{B9}$$

This is represented using the generating functional W

$$I = -ie\widetilde{V}_{\mathrm{C}} \sum_m \int d\omega \left(\frac{\delta}{\delta J_{-;Lm}} \frac{\delta}{\delta \bar{J}_{-;Rm}} - \frac{\delta}{\delta J_{-;Rm}} \frac{\delta}{\delta \bar{J}_{-;Lm}}\right) \exp(W[J_+, J_-]) \tag{B10}$$

$$= -2ie\widetilde{V}_{\mathrm{C}} \int d\omega \left[G_{1,3}(\omega) - G_{3,1}(\omega)\right], \tag{B11}$$

where $G_{n,m}(\omega)$ is the (n, m) component of G. I is finally given by

$$I = 2e \int d\omega\ T(\omega) \left[f_L(\omega) - f_R(\omega)\right] \tag{B12}$$

with $T(\omega)$ in Eq. (13).

To derive Eq. (B12), we have assumed $\widetilde{\Delta}_\alpha$, $\widetilde{E}_\alpha$, and κ are determined by the self-consistent equations for the thermal equilibrium case $\mu_L = \mu_R$. Thus, the present calculation is valid only in the limit of $\mu_L \to \mu_R$. Extensions to the case of finite V_{sd} is possible within the framework of the present method. See Refs. 30,43.

APPENDIX C: KONDO TEMPERATURE WHEN $V_C/\Delta \gg 1$

In this appendix, we derive the gate voltage dependence of $\widetilde{\Delta}$ when $J=0$. The self-consistent equations are given by

$$(\bar{b}_0^2 - 1/2) + \frac{1}{2\pi}\sum_P \mathrm{Im}\left[\ln\left(\frac{\pi\xi_P}{\Delta}\right)\right] = 0, \tag{C1}$$

$$(\widetilde{E} - V_g) + \frac{1}{2\pi}\sum_P \mathrm{Im}\left[(PV_C + i\Delta)\ln\left(\frac{\pi\xi_P}{\Delta}\right)\right] = 0, \tag{C2}$$

where $\xi_P = \widetilde{E} + P\widetilde{V}_{\mathrm{C}} + i\widetilde{\Delta}$ with $\widetilde{V}_C = \bar{b}_0^2 V_C$ and $\widetilde{\Delta} = \bar{b}_0^2\Delta$.

When $V_g < -V_C/2$, the Kondo state is formed in each dot and lead and thus $\widetilde{E} = 0$. Then Eq. (C2) is reduced to

$$-V_g - \frac{V_C}{\pi}\arctan(V_C/\Delta) + \frac{\Delta}{\pi}\ln\left(\frac{\pi\sqrt{\widetilde{\Delta}^2 + \widetilde{V}_{\mathrm{C}}^2}}{\Delta}\right) = 0, \tag{C3}$$

resulting in the first line of Eq. (17).

When $-V_C/2 < V_g < V_C/2$, the broad peak of G appears. For this case, the bonding level is located near the Fermi level in the leads and the antibonding level is far away from the Fermi level. Then we can use the following two conditions: (i) $\widetilde{E} \cong \widetilde{V}_{\mathrm{C}}$ ($\mathrm{Re}\xi_- \cong 0$) and (ii) $\sum_P \mathrm{Im}\left[\ln\left(\frac{\pi\xi_P}{\Delta}\right)\right] \cong -\sum_P \mathrm{Im}\left[P\ln\left(\frac{\pi\xi_P}{\Delta}\right)\right] \cong \mathrm{Im}\left[\ln\left(\frac{\pi\xi_-}{\Delta}\right)\right]$. Then substituting Eq. (C1) into Eq. (C2) yields

$$2\widetilde{V}_{\mathrm{C}} - \left(V_g + \frac{1}{2}V_C\right) + \frac{\Delta}{2\pi}\sum_P \mathrm{Re}\left[\ln\left(\frac{i\pi\widetilde{\Delta}}{\Delta}\right) + \ln\left(\frac{\pi\left(2\widetilde{V}_{\mathrm{C}} + i\widetilde{\Delta}\right)}{\Delta}\right)\right] = 0. \tag{C4}$$

The logarithmic terms are negligible because $n \cong 1$ so that $\widetilde{\Delta} \sim \Delta/2$ and $\widetilde{V}_{\mathrm{C}} \sim V_C/2$. Thus the gate voltage dependence of $\widetilde{\Delta}$ reduces to the second line in Eq. (17).

When $V_C/2 < V_g$ where $n < 1$, the coupled dot system is essentially the same as the noninteracting system; n is determined by the position of the energy level:

$$n = 1 - \frac{2}{\pi}\arctan\left(V_g/\Delta\right). \tag{C5}$$

This result yields the third line of Eq. (17), because $\widetilde{\Delta} = \Delta(1 - n/2)/2$.

Finally, we mention the relation between κ and $\widetilde{\Delta}$ when $J \neq 0$ (Sec. V). The self-consistent equation for κ, Eq. (A16),

$$\frac{2\kappa}{J} + \frac{1}{\pi}\sum_P \mathrm{Im}\left[P\ln\left(\frac{\pi\xi_P}{\Delta}\right)\right] = 0, \tag{C6}$$

is simplified for $-V_C/2 < V_g < V_C/2$. Using the conditions (i) and (ii), we obtain

$$\frac{2\kappa}{J} + \frac{\widetilde{\Delta}}{\Delta} - 1/2 = 0. \tag{C7}$$

---

[1] D. Goldhaber-Gordon, Hadas Shtrikman, D. Mahalu, David Abusch-Magder, U. Meirav and M. A. Kastner, Nature (London) **391**, 156 (1998); D. Goldhaber-Gordon, J. Göres, M. A. Kastner, Hadas Shtrikman, D. Mahalu, and U. Meirav, Phys. Rev. Lett. **81**, 5225 (1998).

[2] S. M. Cronenwett, T. H. Oosterkamp, and L. P. Kouwenhoven, Science **281**, 540 (1998).

[3] J. Schmid, J. Weis, K. Eberl and K. v. Klitzing, Physica B, **256**, 182 (1998).

[4] F. Simmel, R. H. Blick, J. P. Kotthaus, W. Wegscheider, and M. Bichler, Phys. Rev. Lett. **83**, 804 (1999).

[5] L. I. Glazman and M. É. Raĭkh, Pis'ma Zh. Eksp. Teor. Fiz. **47**, 378 (1998). [JETP Lett. **47**,452 (1988).]

[6] T. K. Ng and P. A. Lee, Phys. Rev. Lett. **61**, 1768 (1988).

[7] A. Kawabata, J. Phys. Soc. Jpn. **60**, 3222 (1991).

[8] S. Hershfield, J. H. Davies, and J. W. Wilkins, Phys. Rev. Lett. **67**, 3720 (1991); Phys. Rev. B **46**, 7046 (1992).

[9] Y. Meir, N. S. Wingreen, and P. A. Lee, Phys. Rev. Lett. **70**, 2601 (1993); N. S. Wingreen and Y. Meir, Phys. Rev. B **49**, 11040 (1994).

[10] A. L. Yeyati, A. Martin-Rodero, and F. Flores, Phys. Rev. Lett. **71**, 2991 (1993).

[11] A. Oguri, H. Ishii and T. Saso, Phys. Rev. B **51**, 4715 (1995).

[12] J. König, H. Schoeller, and G. Schön, Phys. Rev. Lett. **76**, 1715 (1996); J. König, J. Schmid, H. Schoeller, and G. Schön, Phys. Rev. B **54**, 16820 (1996).

[13] S. Tarucha, D. G. Austing, T. Honda, R. J. van der Hage, and L. P. Kouwenhoven, Phys. Rev. Lett. **77** , 3613 (1996).

[14] *Mesoscopic Electron Transport* edited by L. L. Sohn, L. P. Kouwenhoven and G. Schön, (Kluwer Academic, Dordrecht, 1997).

[15] D. G. Austing, T. Honda and S. Tarucha, Jpn. J. Appl. Phys. **36**, 1667 (1997).

[16] F. R. Waugh, M. J. Berry, D. J. Mar, R. M. Westervelt, K. L. Campman, and A. C. Gossard, Phys. Rev. Lett. **75**, 705 (1995).

[17] R. H. Blick, D. Pfannkuche, R. J. Haug, K. v. Klitzing, and K. Eberl, Phys. Rev. Lett. **80**, 4032 (1998); R. H. Blick, D. W. van der Weide, R. J. Haug, and K. Eberl, ibid **81**, 689 (1998).

[18] T. H. Oosterkamp, T. Fujisawa, W. G. van der Wiel, K. Ishibashi, R. V. Hijman, S. Tarucha, and L. P. Kouwenhoven, Nature (London) **395**, 873 (1998).

[19] W. Heitler and F. London, Z. Phys. **44**, 455 (1927).

[20] M. Eto, Solid-State Electronics **42**, 1373 (1998).

[21] G. Burkard, D. Loss, and D. P. DiVincenzo, Phys. Rev. B **59**, 2070 (1999).

[22] N. Read and D. M. Newns, J. Phys. C **16**, L1055 (1983).

[23] P. Coleman, Phys. Rev. B **35**, 5072 (1987).

[24] N. E. Bickers, Rev. Mod. Phys. **59**, 845 (1987).

[25] D. M. Newns and N. Read, Adv. Phys. **36**, 799 (1988).

[26] A. C. Hewson, *The Kondo Problem to Heavy Fermions* (Cambridge University Press, Cambridge, 1997).

[27] The local density of states for electrons in the dot is $\rho(\omega) = b_0^2 \rho_f(\omega)$. The transmission probability is $T(\omega) = \widetilde{\Delta}^2/[(\omega - \widetilde{E})^2 + \widetilde{\Delta}^2]$.

[28] F. D. M. Haldane, Phys. Rev. Lett. **40**, 416 (1978).

[29] W. Izumida, O. Sakai and Y. Shimizu, J. Phys. Soc. Jpn. **66**, 717 (1997).

[30] T. Ivanov, Europhys. Lett. **40**, 183 (1997); Phys. Rev. B, **56**, 12339 (1997).

[31] T. Pohjola, J. König, M. M. Salomaa, J. Schmid, H. Schoeller and G. Schön, Europhys. Lett. **40**, 189 (1997).

[32] N. Andrei, G. T, Zimányi and G. Schön, Phys. Rev. B **60**, 5125 (1999).

[33] C.A. Büsser, E.V. Anda, A.L Lima, Maria A. Davidovich, and G. Chiappe, Phys. Rev. B **62**, 9907 (2000).

[34] W. Izumida and O. Sakai, Physica B **284**, 1764 (2000); Phys. Rev. B **62**, 10260 (2000).

[35] T. Aono, M. Eto, and K. Kawamura, J. Phys. Soc. Jpn. **67**, 1860 (1998).

[36] A. Georges and Y. Meir, Phys. Rev. Lett. **82**, 3508 (1999).

[37] B. A. Jones, C. M. Varma, and J. W. Wilkins, Phys. Rev. Lett. **61**, 125 (1988).

[38] B. A. Jones and C. M. Varma, Phys. Rev. B **40**, 324 (1989); B. A. Jones, Physica B **171**, 53 (1991).

[39] B. A. Jones, G. Kotliar, and A. J. Millis, Phys. Rev. B **39**, 3415 (1989).

[40] O. Sakai, Y. Shimizu, and T. Kasuya, Solid State Commun. **75**, 81 (1990).

[41] O. Sakai and Y. Shimizu, J. Phys. Soc. Jpn. **61**, 2333 (1992); **61**, 2348 (1992).

[42] I. Affleck and A. W. W. Ludwig, Phys. Rev. Lett. **68**, 1046 (1992); I. Affleck, A. W. W. Ludwig, and B. A. Jones, Phys. Rev. B **52**, 9528 (1995).

[43] R. Aguado and D. C. Langreth, Phys. Rev. Lett. **85**, 1946 (2000).

[44] T. Aono and M. Eto, J. Low. Temp. Phys. **118**, 401 (2000).

[45] K. Kawamura and T. Aono, Jpn. J. Appl. Phys. **36**, 3951 (1997).

[46] J. Schwinger, J. Math. Phys. **2**, 407 (1961) .

[47] R. Fukuda, M. Sumino, and K. Nomoto, Phys. Rev. A **45**, 3559 (1992).

[48] L. V. Keldysh, Zh. Eksp. Teor. Fiz. **47**, 1515 (1964) [Sov. Phys. JETP **20**, 1018 (1965).]

[49] L. Y. Chen and C. S. Ting, Phys. Rev. B **41** 8533 (1990); **43** 2097 (1991).

[50] N. S. Wingreen, A. -P. Jauho, and Y. Meir, Phys. Rev. B **48**, 8487 (1993) .

[51] A. -P. Jauho, N. S. Wingreen, and Y. Meir, Phys. Rev. B **50** 5528 (1994).

[52] The last two terms on the right-hand side of the Hamiltonian are omitted in the expression of the generating functional, because they do not contribute to the expression of the current.

FIG. 1. A quantum dot dimer connected in series.

FIG. 2. The transmission probability $T(\omega)$ as a function of $(\omega - \widetilde{E})/\widetilde{\Delta}$ with the energy of incident electrons ω, the level position $\widetilde{E}$ and width $\widetilde{\Delta}$ of the Kondo resonance. $E_L = E_R$ and $J = 0$. (a) $V_C/\Delta = 0.3$, (b) 1.0, and (c) 10.0. Arrows indicate the positions of the Fermi level in the leads for several values of the gate voltage V_g/Δ.

FIG. 3. (a) The conductance G versus the gate voltage when $V_C/\Delta = 0.3$. $E_L = E_R$. The dotted and solid lines represent the cases of $J = 0$ and $J/\Delta = 9.0 \times 10^{-4}$ ($U/\Delta = 4 \times 10^2$), respectively. (b) The Kondo resonance width $\widetilde{\Delta}$ (dotted line) and the spin-singlet order parameter κ (solid line) versus the gate voltage for $J/\Delta = 9.0 \times 10^{-4}$. The inset shows G (broken line), $\widetilde{\Delta}$ (dotted line), and κ (solid line) as functions of the gate voltage, near the sharp peak of G.

FIG. 4. (a) The conductance G versus the gate voltage when $V_C/\Delta = 10.0$. $E_L = E_R$. The dotted and solid lines represent the cases of $J = 0$ and $J/\Delta = 1.0$ ($U/\Delta = 4 \times 10^2$), respectively. (b) The Kondo resonance width $\widetilde{\Delta}$ (dotted line) and the spin-singlet order parameter κ (solid line) versus the gate voltage for $J/\Delta = 1.0$.

FIG. 5. The conductance G versus the gate voltage for several values of V_C/Δ from 0.2 to 3.0. $E_L = E_R$. All the curves are vertically offset for clarity.

FIG. 6. The conductance G versus the gate voltage when $V_C/\Delta = 0.3$. For $J = 0$, $\Delta E/\Delta = 0.0$ (thin dotted line) and 2.0 (thick dotted line). For $J/\Delta = 9.0 \times 10^{-4}$ ($U/\Delta = 4 \times 10^2$), $\Delta E/\Delta = 0.0$ (thin solid line) and 2.0 (thick solid line).

FIG. 7. The conductance G versus the gate voltage when $V_C/\Delta = 10.0$. For $J = 0$, $\Delta E/\Delta = 0.0$ (thin dotted line) and 8.0 (thick dotted line). For $J/\Delta = 1.0$ ($U/\Delta = 4 \times 10^2$), $\Delta E/\Delta = 0.0$ (thin solid line) and 8.0(thick solid line).

FIG. 8. The conductance G versus the gate voltage for several values of V_C/Δ from 0.2 to 3.0. $\Delta E/\Delta = 2.0$. All the curves are vertically offset for clarity.

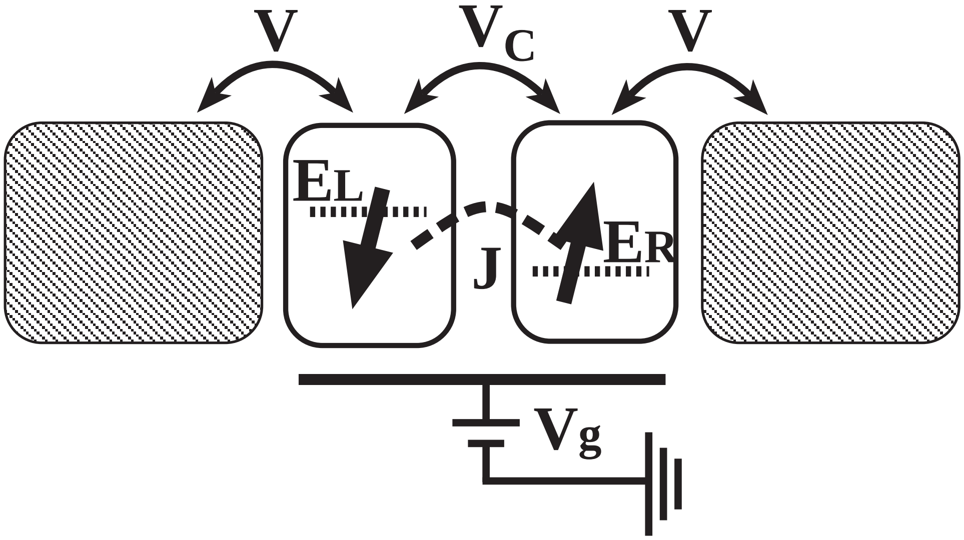

T. Aono and M. Eto, Figure 1

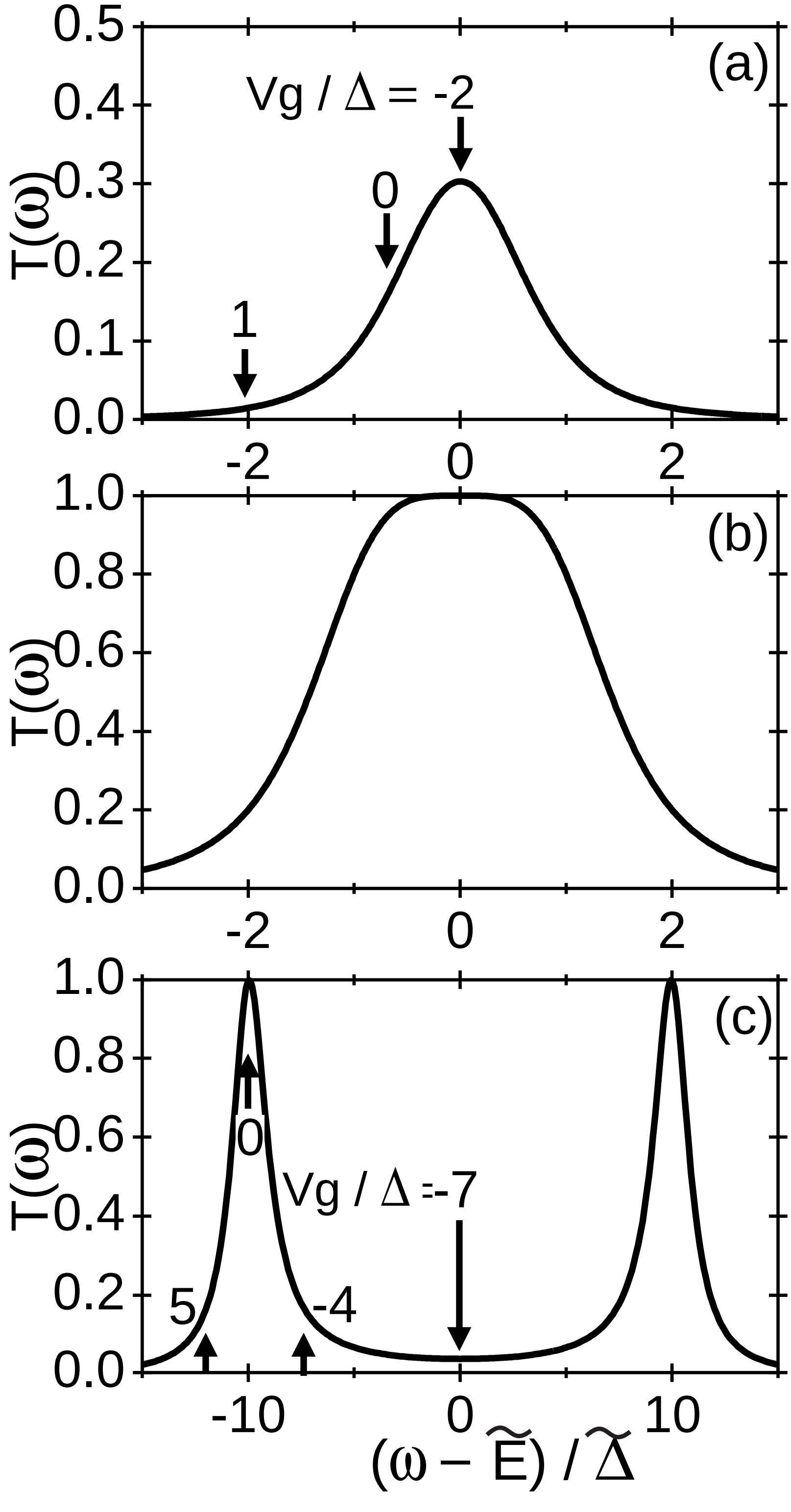

T. Aono and M. Eto, Figure 2

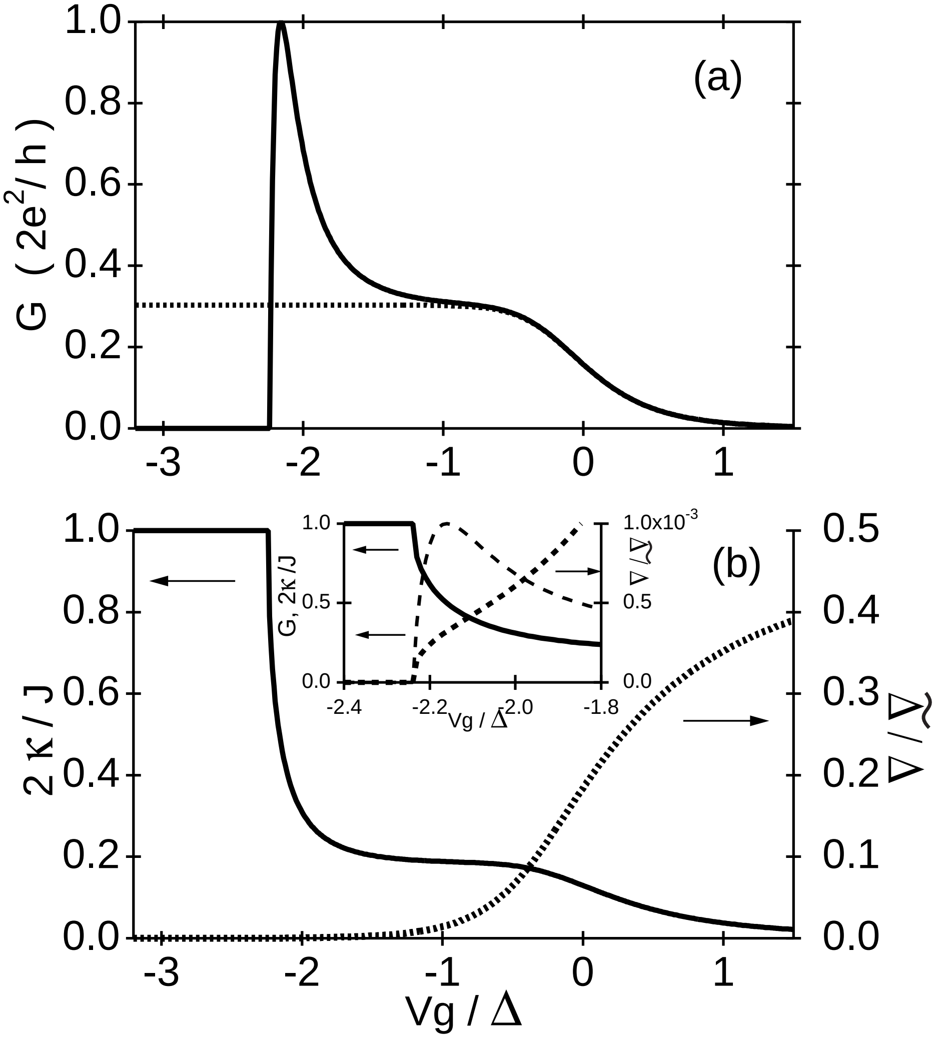

T. Aono and M. Eto, Figure 3

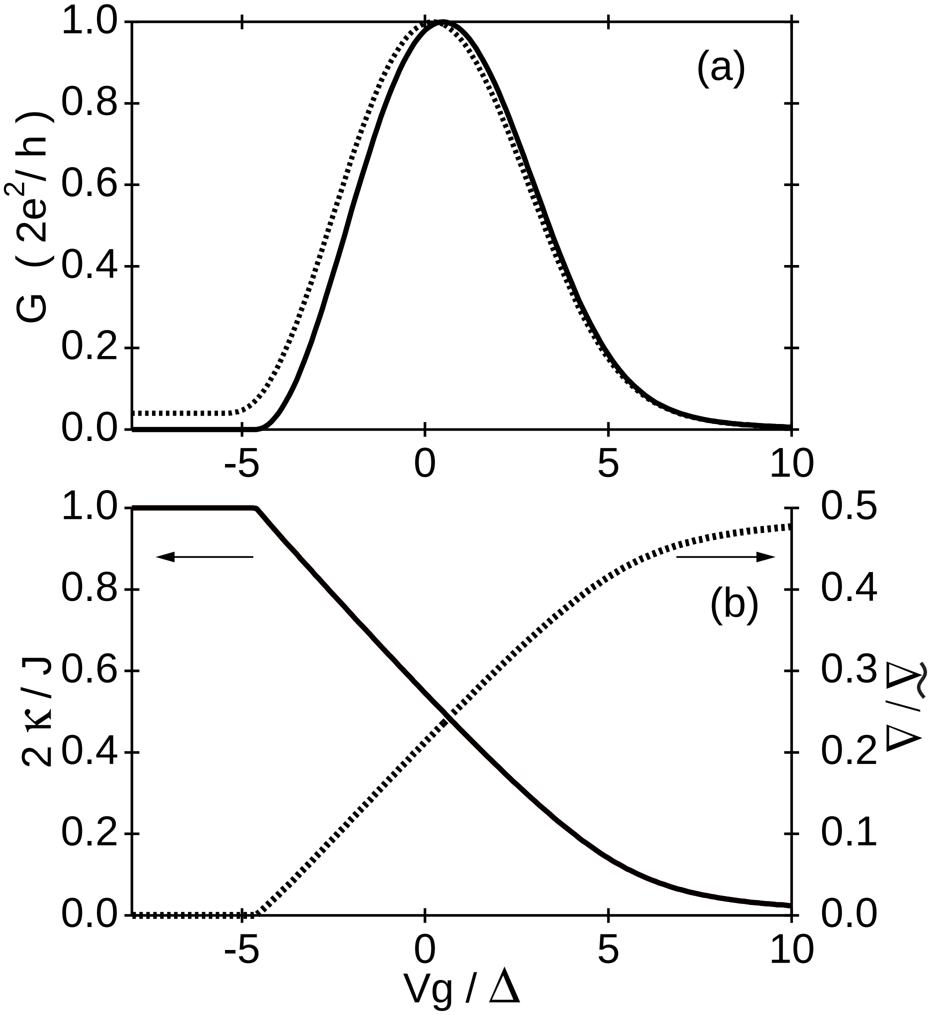

T. Aono and M. Eto, Figure 4

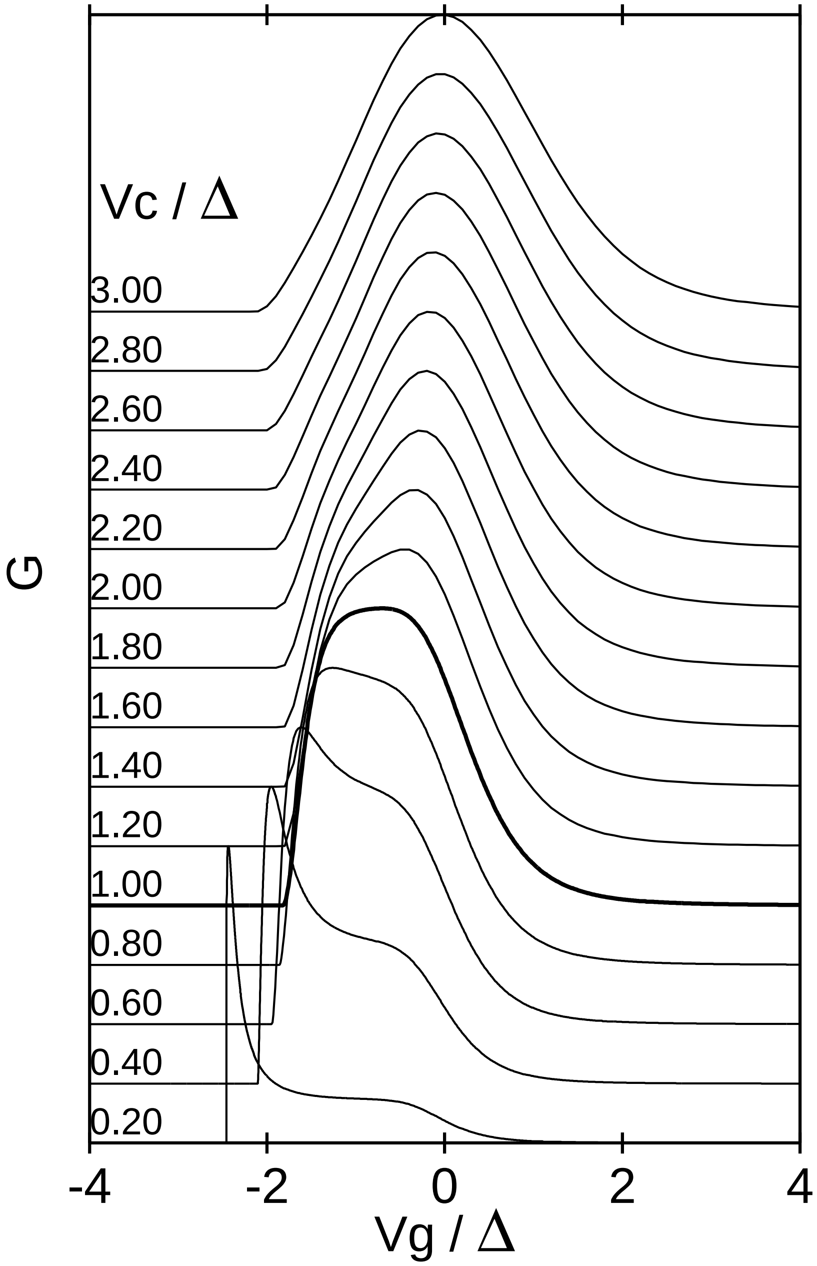

T. Aono and M. Eto, Figure 5

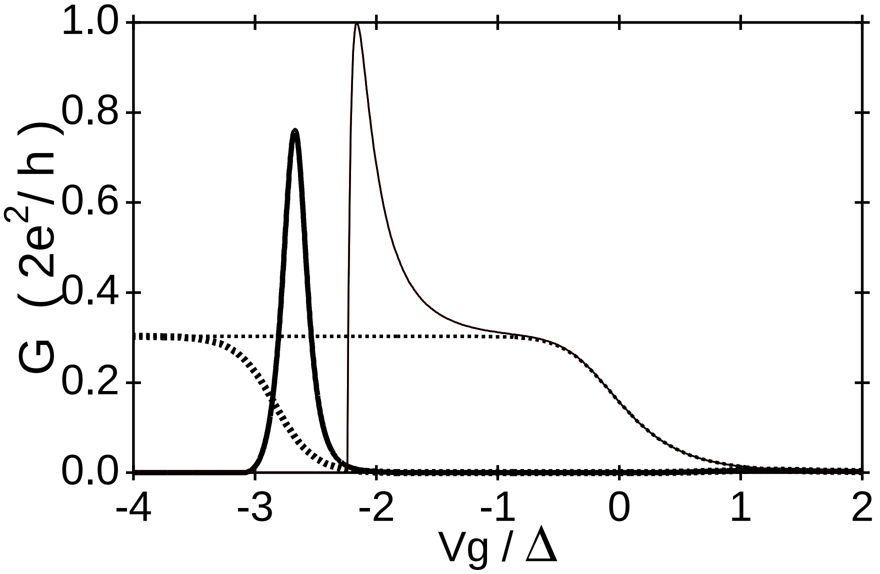

T. Aono and M. Eto, Figure 6

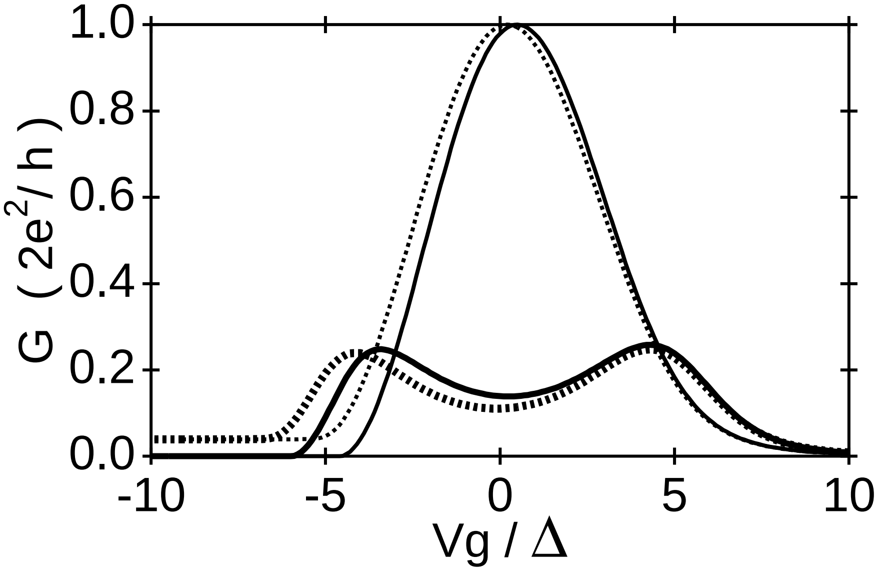

T. Aono and M. Eto, Figure 7

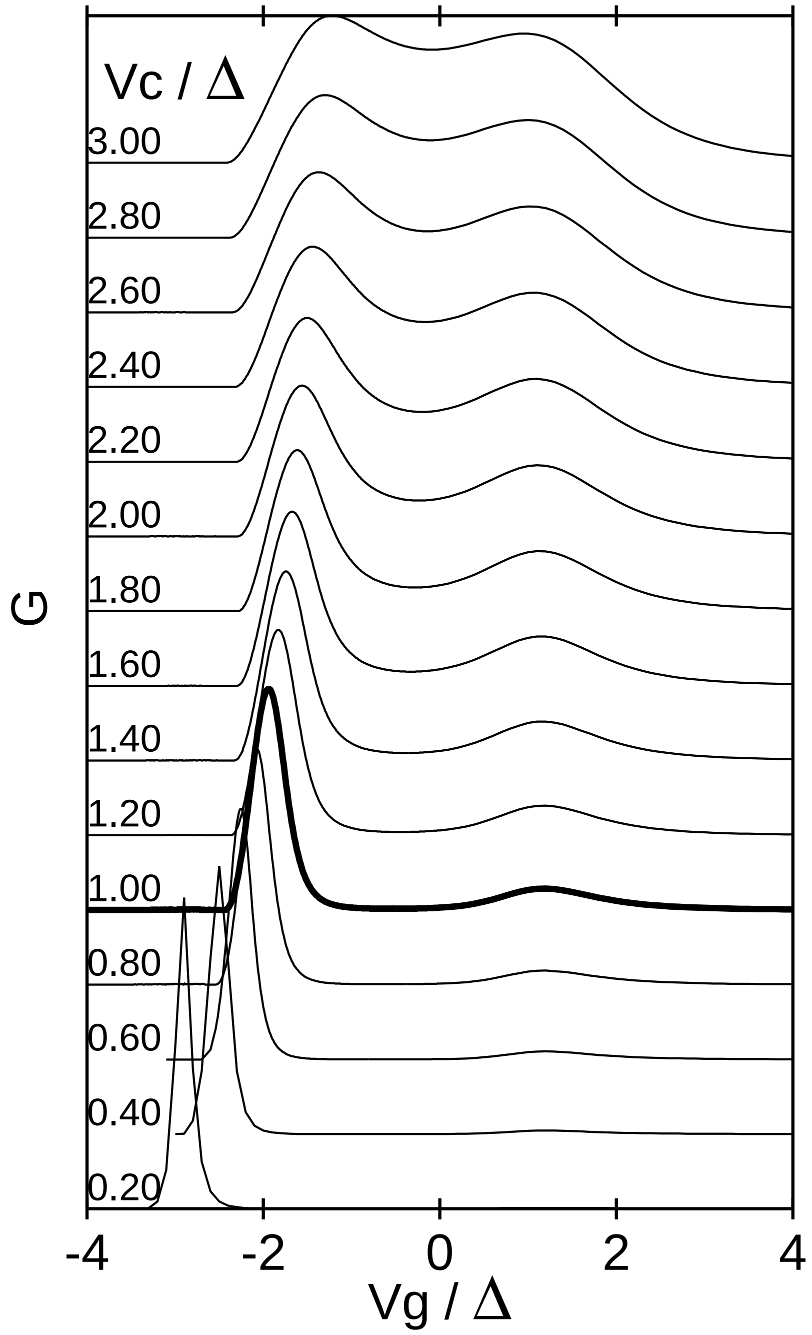

T. Aono and M. Eto, Figure 8